Surface structure of Co–Pd bimetallic particles supported on Al_2O_3 thin films studied using infrared reflection absorption spectroscopy of CO

A. F. Carlsson, M. Bäumer,[a] T. Risse,[b] and H.-J. Freund
Fritz-Haber-Institut der Max-Planck-Gesellschaft, Department of Chemical Physics, Faradayweg 4-6, 14195 Berlin, Germany

(Received 7 July 2003; accepted 26 August 2003)

Infrared reflection absorption spectroscopy of CO has been used as a surface-sensitive probe for the available binding sites of Co–Pd bimetallic particles supported on a thin alumina film. A high-coverage state is obtained on the Co particles in addition to atop sites, attributable to a $M(CO)_n$ species. Bridge and threefold sites are not detected from CO stretching on the Co particles. When both metals are deposited sequentially at 300 K, Pd easily forms a shell on existing Co particles. In the reverse order, much more Co is required to coat Pd particles, because it nucleates between Pd particles as well as on top of them. For both metals, atop sites are better preserved at various bimetallic compositions because they are statistically less vulnerable than threefold hollow sites. The stretching frequency of CO to a given site is nearly independent of the bimetallic composition. © *2003 American Institute of Physics.* [DOI: 10.1063/1.1619943]

I. INTRODUCTION

The conversion of natural gas to liquid fuels is likely to become increasingly attractive as natural gas becomes the transitional energy source in the gradual shift from oil to renewable resources. Environmental pressure to minimize the flaring of natural gas associated with the extraction of crude oil and the use of liquids derived from methane conversion as fuel additives also make the gas to liquid process attractive in the short term. Currently, the gas to liquid (GTL) process is economical only in limited markets, though this is changing with process improvements.[1] The GTL process consists of two major steps: the conversion of natural gas to syngas ($CO+H_2$) and then the conversion of syngas to hydrocarbon liquid fuels through the Fischer–Tropsch reaction.[2]

The direct conversion of methane to higher hydrocarbons[3] and hydrogenation of CO (the Fischer–Tropsch reaction)[4] show greater selectivity and conversion on Co–Pd bimetallic supported catalysts than either metal alone. It has been proposed that the additional Pd facilitates the adsorption of H_2, which spills over and reduces CoO to the more active Co.[3–5] CoO is formed readily at 300 K on close-packed Co(0001).[6] On Co($10\bar{1}0$), ordered structures of adsorbed oxygen are formed,[7] leading to surface reconstructions. In contrast to Co, Pd does not form an oxide as readily.[8]

In the light of the complexity of the processes taking place on such catalysts, well-defined model systems offer the possibility to gain more insight into the microscopic properties. A thin alumina film[9] grown on NiAl(110) has proved to be a suitable model support for these kinds of model systems. The growth and morphology of Pd,[10] Co,[11] and Co–Pd bimetallic[12] particles on this alumina film have previously been studied. Scanning tunneling microscope (STM) images show that at 300 K the majority of Pd particles nucleate and grow at antiphase and reflection domain boundaries on the alumina film.[10] Closer inspection of the triangular-shaped Pd particles has shown the sides and top to be formed by (111) faces.[13] In contrast, pure Co nucleates preferentially at point defects on the alumina film under these conditions, as shown by STM.[14,15] At temperatures above 300 K, where Co atoms on the surface are more mobile, nucleation increasingly occurs at line defects;[11] in general, Co atoms are less mobile than Pd atoms on the alumina substrate due to a stronger metal–substrate interaction.[11] For the preparation of bimetallic particles different preparation schemes are feasible. A deposition of Pd on top of previously deposited Co particles results in a decoration of Co particles by Pd as inferred from STM measurements;[12,16] this is because Pd atoms are mobile enough to reach the more dispersed Co islands. In contrast, reversing the order—namely, evaporation of Co—subsequently to Pd leads to a nucleation of Co metal at point defects between as well as on top of previously deposited Pd particles,[16] because of the lower mobility of the Co atoms. Thus, sequential deposition of Co and Pd results in a core-shell structure, where the second metal deposited forms the shell.

On the pure metals CO prefers different adsorption sites. On Pd, CO is bound preferentially to threefold hollow sites, followed by bridge and finally atop sites;[17] on Co the order is reversed: Co is bound preferentially to atop sites followed by more highly coordinated sites.[18] The interactions of CO with Co–Pd bimetallic particles have been studied recently with TPD.[16] The binding energy of CO to both Pd and Co sites is lowered by the presence of the other metal which can often

[a]Present address: Institut für Angewandte und Physikalische Chemie, Universität Bremen, Postfach 330440, 28334 Bremen, Germany.
[b]Author to whom correspondence should be addressed. Electronic mail: risse@fhi-berlin.mpg.de

 © 2003 American Institute of Physics

Downloaded 28 Mar 2007 to 141.14.132.17. Redistribution subject to AIP license or copyright, see http://jcp.aip.org/jcp/copyright.jsp

be understood on the basis of the so-called ligand effect.[19] The effect is due to a modification of the electronic structure by the exchange of metal in the vicinity of the adsorption site. In addition, CO-atop sites are better preserved at various bimetallic compositions because they are statistically less vulnerable than the Pd threefold hollow sites. This statistical consideration is also known as ensemble effect. A brief calculation based on particle shape indicates that 1.4 Å Co is required to form a complete shell on Pd particles formed by depositing 2 Å Pd, neglecting the additional pure Co nucleating between Pd particles. In the reverse order, 1.2 Å Pd is required to form a complete shell on Co particles formed by depositing 2 Å Co. Herein, the cases where 1 Å of one metal is covering 2 Å of the other were chosen as examples because the second metal is expected to form an incomplete overlayer; under these conditions the most interesting bimetallic effects might be expected.[16]

In this paper we will use infrared reflection absorption spectroscopy (IRAS) of CO as a probe molecule to gain more insight into the adsorption sites present for the various preparation conditions. The paper is organized as follows: After a brief experimental section we will discuss the different preparation conditions separately. The discussion starts with the pure Co situation. After that Pd subsequently deposited on top of Co is discussed followed by the discussion of the reversed order. The large database of IRAS literature used to interpret the results will be reviewed in the course of the discussion. Finally, conclusions will be drawn by comparion of the three situations.

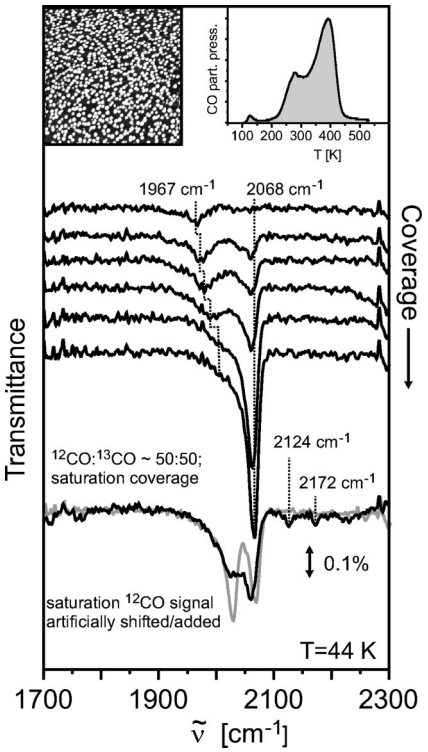

FIG. 1. IR spectra of adsorbed CO on 2 Å Co particles on the alumina film taken at 44 K as a function of CO coverage. The black trace of the bottom panel shows the spectrum resulting from saturation coverage of a 50:50 mixture of ^{13}CO:^{12}CO. The gray trace is a artificially created by adding the saturation coverage spectra ^{12}CO and ^{13}CO scaled by a factor $\frac{1}{2}$. Left inset: STM image of 2 Å Co; 100×100 nm (Ref. 12); right inset: TPD spectrum of 2 Å Co (Ref. 12).

II. EXPERIMENT

The experimental apparatus used in this study has been described in detail elsewhere.[20] The NiAl(110) sample was cleaned by cycles of sputtering and annealing to 1300 K until no impurities were found using AES. The alumina film was prepared by previously described methods[9,10] and the quality of the film was checked using LEED. A triple-metal evaporator (Omicron/Focus EFM 3T) was used to deposit Co and Pd; the average thickness was calibrated with a quartz microbalance *in situ*. The average thickness of the film is herein given in angstroms, where 1 ML is equivalent to 2.035 Å Co or 2.246 Å Pd assuming growth in the close-packed directions of Pd(111) and Co(0001). The notation "2 Å Co particles" will be used to denote an ensemble of Co particles forming an average thickness of 2 Å. Unless otherwise stated, Co and Pd were deposited at room temperature. High-purity CO was passed through a liquid nitrogen trap for further purification before being introduced into the vacuum system.

IRAS spectra were taken with a Bio-Rad spectrometer operating at 4 cm^{-1} resolution with a liquid-nitrogen-cooled MCT detector. Background spectra were collected after depositing the metals and then cooling to 44 K but before exposing the sample to CO. Depending on the flow rate of liquid helium used for cooling, the temperature varied by ±5 K; thus during some experiments CO adsorption on the alumina film was observed, while in others it was not [desorption maxima at ~40 K and ~55 K (Ref. 21)]. During experiments, the chamber pressure was typically 5×10^{-11} mbar, and 1000 scans were accumulated for each spectrum, requiring about 10 min.

III. RESULTS AND DISCUSSION

A. Pure cobalt

IR spectra of various CO coverages adsorbed at 44 K on Co particles corresponding to an average thickness of 2 Å (hereafter referred to as 2 Å Co particles) on the alumina film are shown in Fig. 1. At low coverage, an absorption band appears at 1967 cm^{-1}, attributable to atop-bound CO (Ref. 22); this peak gradually shifts to higher energy with increasing coverage. Just after the adsorption band at 1967 cm^{-1} forms, another band at 2060 cm^{-1} also begins to grow in intensity; this second feature shifts only slightly to 2068 cm^{-1} at saturation coverage and is much stronger than the band due to atop-bound CO at this point. As the absorption band due to atop adsorption shifts to higher energy, it melds into a tail of the absorption feature at 2068 cm^{-1}, making it difficult to quantify the stretching frequency for atop-bound CO at the saturation limit. After annealing to 300 K, the peak attributable to atop-bound CO remains at about 2000 cm^{-1} and the feature at 2068 cm^{-1} vanishes (data not shown). A quantitative evaluation of the IR intensities in correlation with the corresponding TPD results (see inset Fig. 1) reveals a dynamic dipole moment of the species at

Downloaded 28 Mar 2007 to 141.14.132.17. Redistribution subject to AIP license or copyright, see http://jcp.aip.org/jcp/copyright.jsp

2068 cm^{-1}, being by at least a factor of 2 higher as compared to the regular on-top sites. A detailed discussion of this aspect is described elsewhere.[23] The intensity of the on-top signal located around 2015 cm^{-1} at saturation coverage is further reduced by dynamic intensity transfer to the line at 2068 cm^{-1} (Ref. 24). Both effects result in a small intensity of the on-top peak at saturation coverage even though it is the majority species on the surface of the particles.

A variation of particle size and density as prepared by deposition of 0.5 Å Co shows a similar IR absorption band at 2068 cm^{-1} as well as a similar annealing behavior as compared to the 2 Å deposit.

The adsorption band at 2068 cm^{-1} has no counterpart on smooth single-crystal surfaces. There, only redshifted bands (1900–1967 cm^{-1}) were observed which have been assigned to bridge bound species.[22,25] Adsorption bands at 2080 cm^{-1} and 2040 cm^{-1} have been observed for CO adsorbed on sputtered Co(0001) (Ref. 25) and unannealed films (Ref. 26); in the former case this was attributed to CO adsorption at defect sites,[25] and in the latter case it was attributed to carbonyl formation.[26] An adsorption band near 2068 cm^{-1} has also been observed on supported Co particles[27,28] and has been attributed to an $M(CO)_n$ species.[27] The assignment as a single-centered carbonyl is based on analogy with metal carbonyls which suggests the following categorizations:[29] on-top 2000–2130 cm^{-1}, twofold bridge 1860–2000 cm^{-1}, and threefold bridge 1800–1920 cm^{-1}. Given these categories, it seems reasonable to attribute the band at 2068 cm^{-1} to an $M(CO)_n$ species.

Generally, adsorption at defects would be expected to have a higher binding energy, whereas in this case this state desorbs at lower temperature than the regular atop site. This is an indication that the absorption feature at 2068 cm^{-1} is attributable to a carbonyl species.

In an attempt to clarify the nature of the absorption band at 2068 cm^{-1}, isotope exchange experiments have been performed. The pure ^{13}CO case shows a peak at 2022 cm^{-1}, as expected from simple mass considerations predicting the frequency of the ^{13}CO isotope to be lowered by a factor of 0.978. The spectrum of an equimolar mixture of ^{13}CO and ^{12}CO at saturation coverage is shown as the black trace in the bottom panel of Fig. 1. In the case of decoupled oscillators the mixture would result in two bands with equal intensity; this is indeed observed for ^{12}CO and ^{13}CO adsorbed on the alumina film characterized by two bands at 2172 cm^{-1} and 2124 cm^{-1}, respectively (black trace, bottom panel of Fig. 1). In contrast, the absorption band at 2068 cm^{-1} is not split into two well-resolved peaks; only one broad feature is observed in the spectrum. However, the low-energy cutoff is around 2022 cm^{-1}, in line with expectations form simple mass considerations. To visualize the effect expected for simple decoupled oscillators, the experimental spectra of ^{12}CO and ^{13}CO were scaled and added (light trace, bottom panel of Fig. 1). It is clearly seen that the spectrum recorded for the equimolar mixture has an enhanced IR intensity in the intermediate region between the two bands expected for decoupled oscillators. This intensity in the intermediate region is gained at the expense of the low-energy band. This result may be explained either by a dynamic coupling of the CO oscillators which would lead to an intensity transfer from the low-frequency to the high-frequency band[24] or by the formation of carbonyl species $M(CO)_n$ with more than one CO ligand which show additional lines in this region for the various isotope patterns.

The dynamic coupling of the molecules is not sufficient to explain the experimental results. This is based on the following argument: first, an inspection of the mixed spectrum reveals a redshift of the peak at 2068 cm^{-1} by 6 cm^{-1}, indicating a reduction of the coupling of these species with neighboring sites as expected for a dilution of ^{12}CO by ^{13}CO. On the other hand, the intensity enhancement in the intermediate region around 2040 cm^{-1} would require a pronounced intensity borrowing from species absorbing below this range. Clearly, the ^{13}CO counterpart absorbing at 2022 cm^{-1} could account for the intensity borrowing, in principle. However, this is in contradiction with the reduced coupling to the ^{12}CO species at 2068 cm^{-1} with its neighbors, because the neighbors are identical species and the coupling between them was independently shown by quantitative analysis of the IR data in combination with the TPD. Therefore, dynamic coupling of CO molecules is an unlikely explanation for the observed phenomena. It is, however, likely that dynamic coupling plays a role for the relative intensities of the observed peaks.

On the other hand, carbonyl formation is a well-known phenomenon in Co chemistry. The most stable Co carbonyl is Co_2CO_8 but also monometal carbonyls [$Co(CO)_n$ with $n=1-4$] are known from matrix isolation studies.[30] Referring to the previous discussion it is obvious that the carbonyl species $Co(CO)_n$ has to have more than one CO ligand to show additional lines in the intermediate region. From a chemical point of view the formation of a multinuclear carbonyl species requires Co atoms with low metal–metal coordination as compared to regular low-index surfaces. The presence of such sites is compatible with the noncrystalline nature of the cobalt deposits.[12] A determination of the stoichiometry is hampered by the unknown symmetry of the carbonyl species as well as possible intensity borrowing effects which renders a prediction of the expected intensity profile challenging. Therefore, two additional experiments have been performed to elucidate this problem further. Here 30 L (1 L$=10^{-6}$ Torr s) of ^{12}CO (saturation) were dosed at 44 K to 2 Å of Co. This sample was annealed to 295 K, resulting in the loss of the peak at 2068 cm^{-1} as described above. It was cooled down to 44 K again and redosed with ^{13}CO to saturation. The observed spectrum shows an asymmetric peak at 2033 cm^{-1} (data not shown). The same experiment was done starting with ^{13}CO, subsequent annealing, and redosage with ^{12}CO. This preparation shows an asymmetric peak at 2056 cm^{-1}. The shift of the IR frequencies by 11 and 12 cm^{-1} as compared to the pure isotopic spectra can be understood if one assumes a decomposition of the multinuclear carbonyl upon annealing while a single CO molecule remains adsorbed on the site. A readsorption of the other isotope would result in species $^{12}Co_{n-1}\,^{13}Co$ and $^{13}Co_{n-1}\,^{12}Co$, respectively. Taking the difference in frequency between $^{12}Co_n$ and $^{12}Co_{n-1}\,^{13}Co$ (11 cm^{-1}) as well as $^{13}Co_n$ and $^{13}Co_{n-1}\,^{12}Co$ (12 cm^{-1}), comparisons with the frequency differences and the corresponding amount of ex-

Downloaded 28 Mar 2007 to 141.14.132.17. Redistribution subject to AIP license or copyright, see http://jcp.aip.org/jcp/copyright.jsp

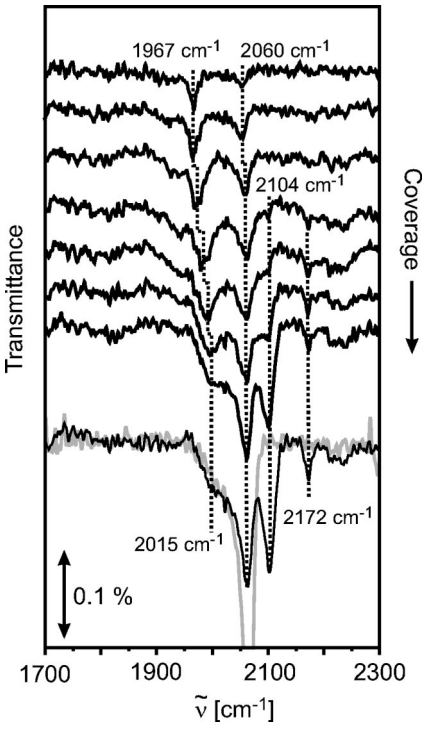

FIG. 2. IR spectra of adsorbed CO on 2 Å Co particles with subsequently deposited 0.1 Å Pd on the alumina film taken at 44 K as a function of CO coverage. The IR spectrum at saturation coverage of pure Co (2 Å) is shown for comparison (gray trace) in the bottom panel.

pected lines in matrix isolated carbonyls suggest a stoichiometry of $n=4$. However, a stoichiometry with $n=3$ cannot be excluded completely on the basis of the experimental data. Therefore, the stoichiometry of the carbonyl is $n \geqslant 3$.

Originally, the first peak in the TPD of CO from 2 Å Co particles at 280 K was assigned to desorption from bridge sites due to the coincidence of the desorption temperature with that for bridge sites observed on single crystal surfaces.[16] However, no feature for Co-bridge sites is observed in the IR. Since the $Co(CO)_n$ species is desorbed upon annealing to 300 K, it now appears more likely that the desorption feature at 280 K is due to the depopulation of $Co(CO)_n$ species. The assignment of the desorption peak at 393 K to Co-atop sites is consistent with the IR data.[16]

B. Palladium on top of cobalt

When only 0.1 Å Pd is subsequently deposited on top of 2 Å Co particles, new features appear in the IR spectrum of adsorbed CO in addition to those of the pure Co particles (Fig. 2). Similarly to the case for pure Co particles, at low coverage, an absorption band at 1967 cm^{-1} appears due to atop-bound CO on Co, shifting to higher energy with increasing coverage. Concurrently, a band at 2060 cm^{-1} appears due to $M(CO)_n$ species on Co. The shoulder at 2015 cm^{-1} on the peak at 2060 cm^{-1} is most likely due to CO adsorption on Co-atop sites, shifted to higher wave numbers at the higher coverage; this feature is also present in the pure Co case, but is not as pronounced. The reason for the relatively small intensity of this feature was already discussed in the previous section. The new feature arises at higher coverage: a band at 2104 cm^{-1} begins to grow in and becomes quite clear at saturation coverage. Due to the good agreement with values from the literature,[10] we attribute the band at 2104 cm^{-1} to atop-bound CO on Pd. Finally, there is a band at 2172 cm^{-1} attributable to CO adsorbed on the alumina film; this feature can be desorbed by heating to 60 K and repopulated again at 44 K. Interestingly, the CO is preferentially bound to the metal particles at low coverage before populating the film, suggesting, as we might expect, high mobility of CO molecules on the film at 44 K.

Although Pd threefold sites have a higher binding energy, only atop sites can be populated on the 2 Å Co $+0.1$ Å Pd, because threefold sites are statistically more difficult to form at low Pd coverage. A comparison of the spectra obtained at saturation coverage for pure 2 Å Co (gray trace, Fig. 2) and 2 Å Co$+0.1$ Å Pd (bottom panel, Fig. 2) shows that the growth of the new peak associated with Pd atop species is completely at the expense of the Co carbonyl species. Therefore, it can be concluded that the low-coordinated Co atoms which form the carbonyl species in the pure Co case serve as nucleation sites for the adsoption of Pd atoms. The $Co(CO)_n$ species is formed at low-coordinated metal atoms; thus the Pd atoms are also characterized by a reduced metal–metal coordination as compared to closed packed surfaces. A detailed evaluation of the IR intensities in comparison with TPD results shows that the intensity of the Pd atop band is enhanced by a factor of 3 as compared to the Co absorptions.[23] The physical basis of this enhancement is the different response of the metal particle depending on the local environment of the metal atom as is corroborated by density functional theory (DFT) calculations.[23] The additional population of Pd-atop sites does not affect the temperature-programmed desorption spectrum significantly; it is basically the same as that from pure 2 Å Co with the exception that the low-temperature tail is broader for the bimetallic case.[12] This low-temperature shoulder is due to the Pd atop sites which can be shown by temperature-dependent IR spectra.[23]

When 1 Å Pd is subsequently deposited on top of 2 Å Co particles, the IR spectrum is nearly identical to that for pure 2 Å Pd particles (Fig. 3). At low CO coverage, bands at 1838 cm^{-1} and 1930 cm^{-1} attributable to CO bound to Pd threefold and Pd(111)-bridge sites, respectively.[10] Note that the signal due to the Pd threefold hollow sites (1838 cm^{-1}) is unexpectedly broad as compared to the pure Pd particles.[10,31] At slightly higher coverage, bands attributable to CO bound to Pd(100) bridges and particle edges (1980 cm^{-1}) and atop-bound CO (2106 cm^{-1}) appear.[10,31] The spectrum obtained at saturation coverage is almost identical to a spectrum taken for 2.2 Å Pd deposited at 90 K.[31] At a growth temperature of 90 K the island density of Pd is comparable to Co grown at 300 K. Additionally, Pd does not form well-faceted particles under these conditions similar to Co at 300 K. Therefore, the coverage of disordered Co particles by 1 Å Pd at 300 K can result in a similar situation as far as possible binding sites are concerned. However, a simple calculation based on the particle shapes and sizes from STM (Ref. 16) suggests that 1 Å Pd is not enough to fully cover the 2 Å Co particles; thus some evidence of CO

Downloaded 28 Mar 2007 to 141.14.132.17. Redistribution subject to AIP license or copyright, see http://jcp.aip.org/jcp/copyright.jsp

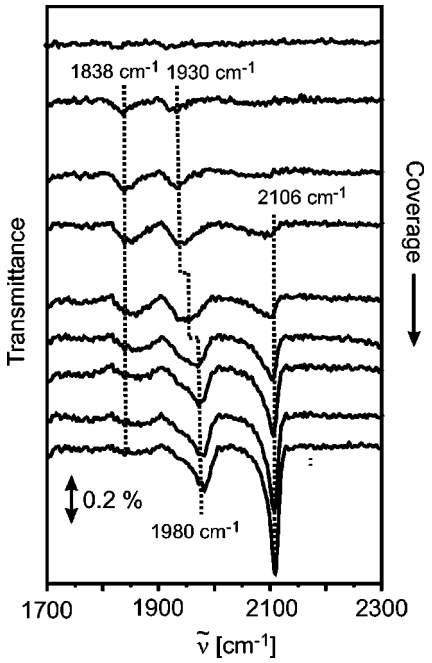

FIG. 3. IR spectra of adsorbed CO on 2 Å Co particles with subsequently deposited 1 Å Pd on the alumina film taken at 44 K as a function of CO coverage.

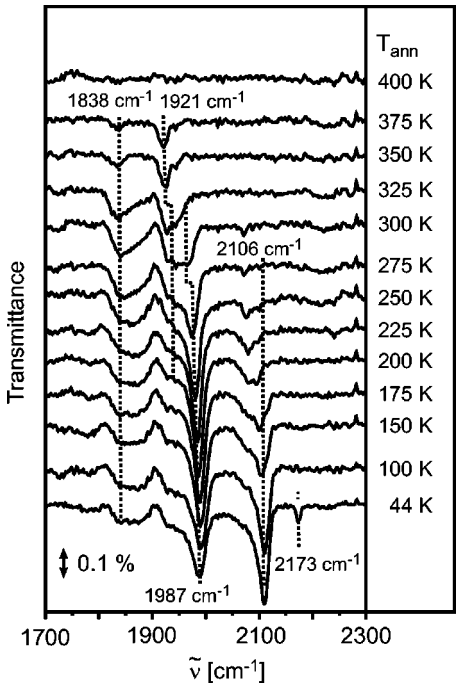

FIG. 4. IR spectra of adsorbed CO on 2 Å Co particles with subsequently deposited 1 Å Pd on the alumina film taken at 44 K as a function of temperature. The sample was exposed to CO at 44 K until saturated and then annealed to the various temperatures; all spectra were taken at 44 K.

on Co-atop sites might be expected at 1967–2000 cm^{-1}. The band due to CO adsorption on Co-atop sites is not obvious, perhaps because it is small in intensity even on the pure 2 Å Co particles or because it is convoluted with the band due to Pd-bridge sites at 1980 cm^{-1}.

A series of IR spectra after annealing to various temperatures is shown for 2 Å Co particles with 1 Å Pd on top in Fig. 4. Due to the $\pm 5\%$ error in amount of metal deposition and the sensitivity of the peak intensities to the bimetallic composition, the peak intensity ratios are slightly different in Figs. 4 and 5. Starting from saturation coverage at 44 K, annealing to higher temperature results in a decrease of the band assigned to Pd-atop sites. The band shifts to lower energy as the population is lowered, until at 275 K the Pd-atop sites are fully depopulated. Concomitantly, the intensity of the peak at 1987 cm^{-1} increases in intensity. A similar intensity redistribution was observed on Pd particles grown at 90 K; however, the desorption temperature of the on-top sites was higher by about 50 K.[31] A shift in frequency with increasing coverage is also observed at constant temperature (Fig. 3), though the shift is much larger in the temperature series, possibly due to a lack of mobility at lower temperatures. The Pd threefold sites (1838 cm^{-1}) remain populated until 375 K. The high-energy side of the corresponding band decreases in intensity as the band becomes sharper at higher temperature; the cause for this sharpening is unclear. The Pd(100)-bridge and edge sites clearly remain populated until 275 K without much shift in the CO stretching frequency. Above 275 K only the Pd(111)-bridge sites remain populated, shifting down to 1921 cm^{-1} and remaining populated until 375 K. The Pd(111)-bridge sites were also observed to remain populated up to this temperature on pure Pd particles while the peak at 1980 cm^{-1} is more stable by at least 70 K in the pure Pd case.[31] In the temperature series, as in the coverage series (Fig. 3), a band due to CO adsorption on Co-atop sites is not obvious, although it is expected; the intensity may simply be too small, or it may be convoluted with the signals attributable to Pd-bridge sites. The TPD spectrum of CO from these particles has one small peak around 190 K,[16] which we can now attribute to desorption from Pd-atop sites, and a broader peak at about 340 K. The broader peak can most likely be attributed to CO desorption from both Co-atop and Pd threefold sites, though no conclusion can be drawn about their relative abundance.

The subsequent deposition of 3 Å Pd on top of 2 Å Co particles shows IR spectra evolving similarly to pure 2 Å Pd with increasing CO coverage (data not shown), thus suggesting that this amount is sufficient to cover the Co particles completely. Even at this full coverage, the TPD peak from Pd threefold sites is shifted to lower temperature due to the underlying Co particles.[16]

C. Cobalt on top of palladium

When only 0.1 Å Co is deposited on top of 2 Å Pd particles, the IR spectrum (Fig. 5) appears similar to pure Pd.[10,31] At low coverage, bands attributable to Pd threefold (1811 cm^{-1}) and Pd(111) bridges (1915 cm^{-1}) appear. With increasing coverage, the band due to CO adsorption in Pd threefold sites disappears and the feature attributable to CO in Pd(111) bridges shifts to 1950 cm^{-1}. Concurrently, new features grow in, attributable to CO in Pd(100) bridges and particle edges (1986 cm^{-1}) and Pd-atop (2106 cm^{-1}) sites. In the intermediate-coverage regime the spectra show relatively broad features which would be consistent with spectral

Downloaded 28 Mar 2007 to 141.14.132.17. Redistribution subject to AIP license or copyright, see http://jcp.aip.org/jcp/copyright.jsp

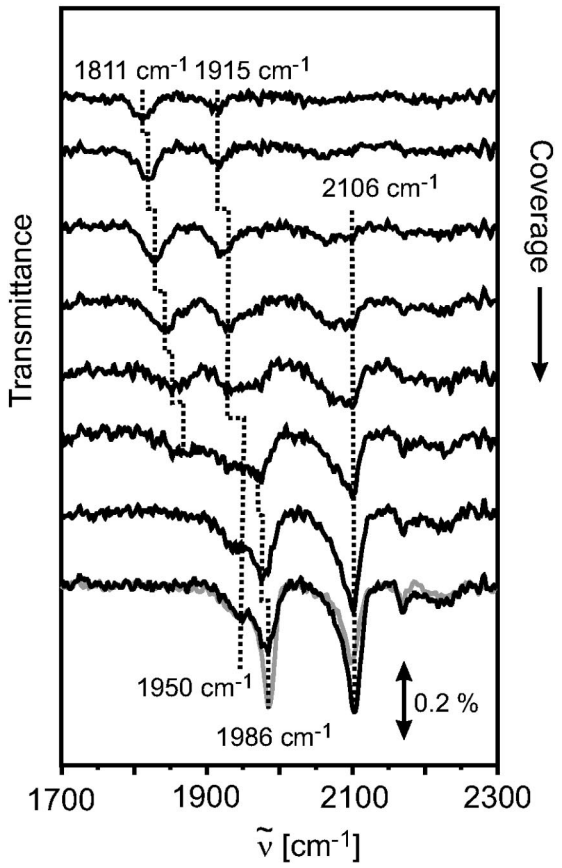

FIG. 5. IR spectra of adsorbed CO on 2 Å Pd particles with subsequently deposited 0.1 Å Co on the alumina film taken at 44 K as a function of CO coverage. The IR spectrum at saturation coverage of pure Pd (2 Å) is shown for comparison (gray trace) in the bottom panel.

components around 2068 cm^{-1} and 1970 cm^{-1} arising from adsorption to Co sites. However, at saturation coverage none of the characteristic Co features is present to an appreciable amount as judged by a comparison of the spectrum of the bimetallic system shown as the black trace in the bottom panel of Fig. 5 and the spectrum of 2 Å Pd particles (gray trace). From STM images it can be concluded that only 10% of the Co atoms nucleate in pure Co particles in between the Pd islands.[12] This small amount may not be expected to contribute much intensity to the spectrum. The remaining 90% of Co leads to an average number of 60 Co atoms per Pd particle. This amount would be sufficient for a 10%–20% coverage of the surface with Co atoms, as calculated from the average number of atoms per Pd island (about 2500 atoms/particle) and the growth mode of these particles.[11,13] This amount should result in an IR signal of atop bound CO molecules from Co sites. However, the stretching frequency of CO adsorbed atop to Co is expected to be located between 1970 and 2000 cm^{-1} and thus convoluted by the absorption band at 1986 cm^{-1} due to Pd(100)-bridge/particle-edge sites. In comparison to the pure Pd case the addition of 0.1 Å Co leads to a decrease of the band at 1986 cm^{-1} and a concomitant increase of the intensity of the peak at 2106 cm^{-1}, while the band at 1950 cm^{-1} associated with Pd(111) bridge sites is virtually unchanged. In case the band at 1986 cm^{-1} would be a convolution of signals stemming from Co atop sites and corresponding Pd sites [particle edges/Pd(100) bridge sites], most of the adsorbed Co atoms would have to decorate these sites to account for the reduced intensity of the peak at 1986 cm^{-1}.

On the other hand, the corresponding TPD spectrum indicates a reduction of the desorption temperature associated with threefold hollow sites from 444 K to 417 K.[16] This indicates that basically all Pd(111) hollow sites are influenced by the additional Co deposition, although they are not depleted, yet. Thus, the largest fraction of the particle surface—namely, the (111) facets—is influenced by Co atoms. Additionally, the x-ray photoemission spectroscopy (XPS) spectrum shows a shift of the Pd 3*d* levels to higher binding energy upon addition of 0.1 Å Co.[16] This result suggests an influence of the Co atoms on the entire island and not just on the surface of the particle.

The experimental results can be explained by assuming that Co is going subsurface. First, it is well known that Pd has the tendency to diffuse to the surface in this bimetallic system[32] and experiments with much larger Co amounts, discussed later on, indicate that interdiffusion occurs in this particular system already at 300 K.

Second, the lack of surface Co atoms would explain the absence of an IR band associated with Co, even though the band at 1986 cm^{-1} can accommodate for some Co atoms being present on the surface. Third, Co atoms located in subsurface layers can still influence the binding energy of CO in the hollow positions via ligand effects, while the surface atoms remain the same. A corresponding shift of the desorption peak of threefold hollow sites was observed for 3 Å Pd deposited on top 2 Å Co where ''subsurface'' Co atoms are present due to the core shell structure of the deposits. Additionally, the number of Pd atoms in direct contact with Co atoms would increase drastically with Co diffusing into deeper layers which helps to explain the XPS result. The increase of the atop peak at 2106 cm^{-1} at the expense of the band at 1986 cm^{-1} which is attributed to particle edges as well as bridge sites on Pd(100) facet can be understood in terms of the growth process. In case interdiffusion of atoms occurs during the growth this will be most probably happen at low-coordinated sites—namely, the edges of the well-faceted particles—which render these sites the most vulnerable to changes during the Co growth.

Upon increase of the Co amount to 1 Å on top of 2 Å Pd, bands from both Co and Pd sites are observed (Fig. 6). At low CO coverage, bands attributable to Pd(111)-bridge (1924 cm^{-1}) and Co-atop (1973 cm^{-1}) sites are observed. At higher coverage, bands attributable to an $M(CO)_n$ species on Co (2064 cm^{-1}) and Pd-atop (2104 cm^{-1}) species are observed. The broad band at 2002 cm^{-1} arising at high CO coverage may be explained by a superposition of Pd(100)-bridge and edge sites and Co-atop sites. Interestingly, at this Co coverage, there is still enough bare Pd for Pd-atop sites to be populated, whereas the Pd threefold sites are already depleted, supporting earlier conclusions based on the ensemble effect that atop sites are more easily preserved upon the formation of bimetallic particles than threefold sites.[16] Again, the subsequent deposition of Co on top of Pd particles leads to the formation of pure Co particles nucleating between the

Downloaded 28 Mar 2007 to 141.14.132.17. Redistribution subject to AIP license or copyright, see http://jcp.aip.org/jcp/copyright.jsp

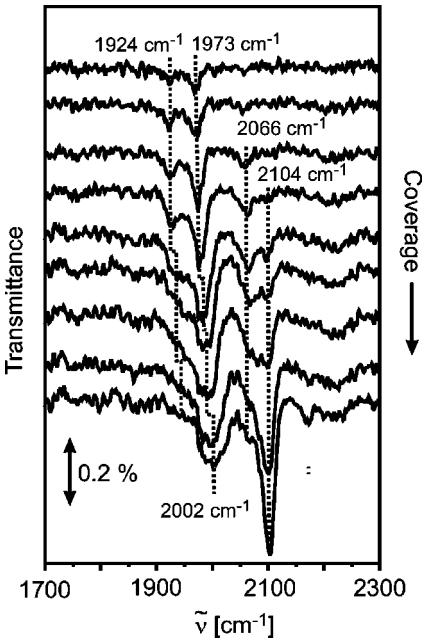

FIG. 6. IR spectra of adsorbed CO on 2 Å Pd particles with subsequently deposited 1 Å Co on the alumina film taken at 44 K as a function of CO coverage.

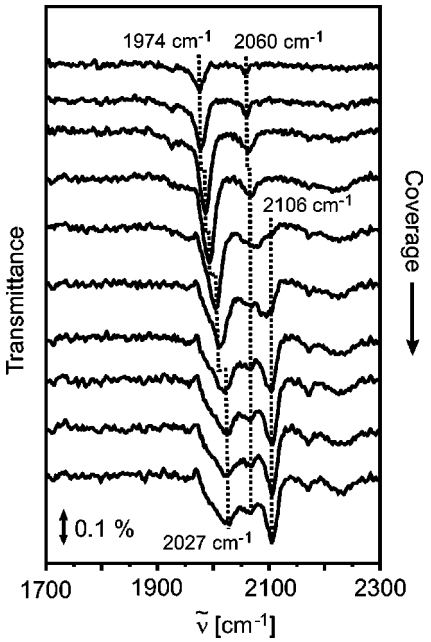

FIG. 8. IR spectra of adsorbed CO on 2 Å Pd particles with subsequently deposited 3 Å Co on the alumina film taken at 44 K as a function of CO coverage.

Pd particles at point defects on the alumina film;[16] at saturation coverage the pure Co particles are known to show a single asymmetric line around 2066 cm^{-1}. An estimate of the ratio of pure Co particles in the bimetallic case as compared to the pure Co situation from STM measurements and the corresponding IR intensity expected for the amount of pure Co particles reveals that the peak at 2066 cm^{-1} is largely due to pure Co particles.

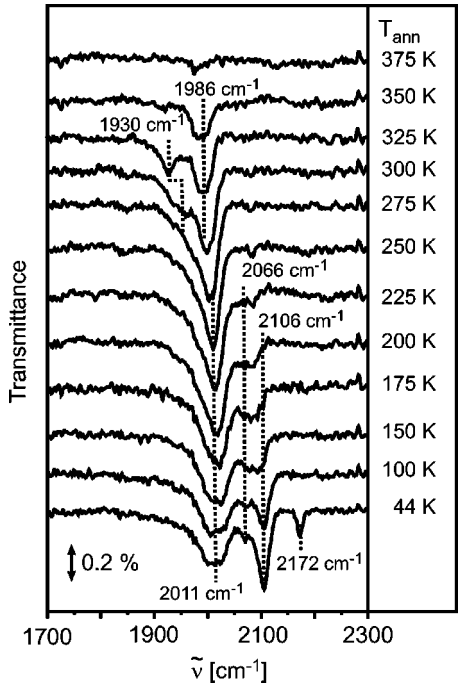

FIG. 7. IR spectra of adsorbed CO on 2 Å Pd particles with subsequently deposited 1 Å Co on the alumina film taken at 44 K as a function of temperature. The sample was exposed to CO at 44 K until saturated and then annealed to the various temperatures; all spectra were taken at 44 K.

A series of IR spectra after annealing to various temperatures is shown for same preparation in Fig. 7. At 44 K all sites are populated as discussed above. After annealing to 250 K, the bands attributable to Pd-atop sites (2106 cm^{-1}) and $M(CO)_n$ species on Co are fully depopulated. Concomitantly, the peak at 2010 cm^{-1} becomes sharper. Annealing to 300 K causes the line at 2010 cm^{-1} to split into a low-energy feature at 1930 cm^{-1} attributable to Pd(111)-bridge sites and a peak at 1986 cm^{-1} attributable to Co-atop sites or Pd(100)-bridge/particle-edge sites. The former desorbs upon annealing to 350 K while the latter sustains up to 350 K and desorbs by 375 K. Taking the intensity redistribution observed for small Co amounts on Pd into account (see Fig. 5) the line at 1986 cm^{-1} is most likely due to Co atop sites. The TPD spectrum of CO from these particles[16] has a broad shoulder increasing in intensity in the range from 110 to 300 K, which we can now attribute to desorption from Pd-atop, $Co(CO)_n$, and Pd-bridge species. The main peak in the TPD spectrum centered at 350 K is most likely due to CO bound to Co-atop sites. Pd threefold sites are not observed, presumably because they are more statistically vulnerable to additions of Co than atop sites.

A further increase of the amount of Co to 3 Å subsequently deposited on top of 2 Å Pd particles shows a superposition of IR signal from both Pd and Co sites, suggesting that 3 Å Co are not sufficient to fully cover the 2 Å Pd particles (Fig. 8). At low coverage, a band attributable to CO adsorption on Co-atop sites appears at 1974 cm^{-1}, along with a band attributable to $Co(CO)_n$ species at 2060 cm^{-1}. There might be a small feature around 1930 cm^{-1} which shifts to towards 1950 cm^{-1} for intermediate coverage, indicating small amounts of Pd(111)-bridge sites. At high cover-

Downloaded 28 Mar 2007 to 141.14.132.17. Redistribution subject to AIP license or copyright, see http://jcp.aip.org/jcp/copyright.jsp

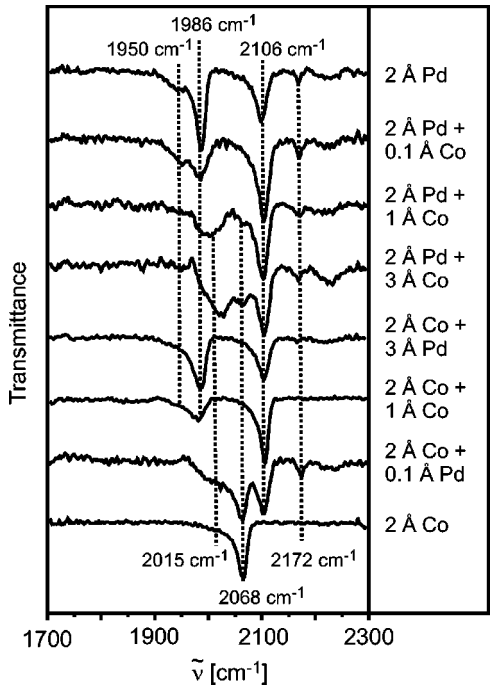

FIG. 9. IR spectra of CO adsorbed on various Co–Pd bimetallic particles supported on an alumina thin film. The designation 2 Å Co+1 Å Pd designates a subsequent deposition of 2 Å Co and then 1 Å Pd at 300 K. Spectra were taken at 44 K.

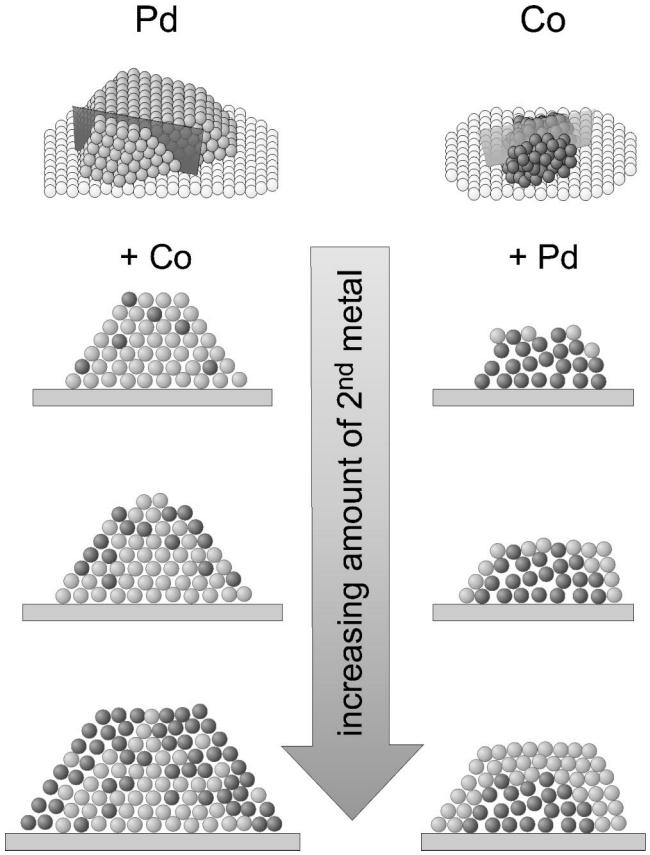

FIG. 10. Schematic representation of the growth mode as inferred from IRAS, TPD, XPS, and STM data (Ref. 16).

age the poor signal-to-noise ratio of the spectra prevents a definite statement about the presence of these species. While the band due to Co-atop sites shifts to higher energy with increasing CO coverage, the band attributable to $Co(CO)_n$ species does not shift appreciably through saturation coverage. At higher coverage, a band at 2106 cm^{-1} appears which is attributable to Pd-atop sites. It is interesting that at such a high coverage of Co is still not able to fully coat the Pd particles.

Additional experiments were performed to test whether Pd segregates to the top when covered by Co or if the difficulty of Co to coat Pd is simply a geometrical effect. When Pd is deposited at 90 K on the alumina film (imaged using STM at 300 K), it nucleates at point defects as well as line defects,[15] because of the lower mobility at 90 K as compared to room temperature. Here 1 Å Pd was deposited at 90 K, and subsequently 5 Å Co was deposited at 300 K, where it can be assumed that most of the Co will nucleate on top of the more strongly dispersed Pd particles; this resulted in IR spectra of adsorbed CO showing both the Co-atop and $Co(CO)_n$ sites, but also Pd-atop sites (data not shown). Evidently this large amount of Co was not able to fully cover even the more finely dispersed Pd particles. The Pd-atop site was still visible when 10 Å Co was deposited at 300 K on top of 1 Å Pd particles deposited at 90 K. However, when a surface of 1 Å Pd particles deposited at 90 K was subsequently covered with 20 Å Co, only the Co-atop and $Co(CO)_n$ sites were observed (data not shown). This suggests that some fraction of the topmost Pd layer on a particle exchanges with the Co as it is deposited on the particle. With every subsequently grown layer, the remaining Pd available for exchange is less, and by the time 20 Å Co are deposited, it is no longer detectable. On the other hand, if Pd naturally segregated to the surface of particles at 300 K via bulk diffusion, we would expect to detect CO adsorption on Pd atop sites even if 20 Å Co are deposited on top of the original Pd particles. Surface segregation in Co–Pd alloys has been detected only at temperatures above 573 K.[32]

Figure 9 shows a collection of IR spectra for various bimetallic compositions at saturation coverage of CO. First, the absorption band attributable to $Co(CO)_n$ species at 2068 cm^{-1} characteristic of the saturation coverage of pure Co particles survives only the addition of 0.1 Å Pd. However, a closer inspection of the spectra revealed that the newly formed signal at 2104 cm^{-1} that is due to Pd-atop sites growing at the expense of the carbonyl feature. An increase of the Pd amount to 1 Å Pd deplete the carbonyl feature completely from the IR spectrum. At first glance, it also appears as if the Co-atop site does not survive 1 Å Pd coverage either, though we know from the temperature series (Fig. 4) that this is not true—indeed Co-atop sites do survive, although they may not be apparent at 44 K because they are convoluted with Pd-bridge sites. Increasing the Pd amount further to 3 Å results in an almost pure Pd behavior as far as the IR spectra goes. This process—namely, the formation of the Pd shell on top of Co particles—is schematically shown in the right panel of Fig. 10.

Co-atop sites are also difficult to discern when Co is covering Pd particles; at low coverage this is partly due to the tendency of Pd to segregate to the surface of a bimetallic

Downloaded 28 Mar 2007 to 141.14.132.17. Redistribution subject to AIP license or copyright, see http://jcp.aip.org/jcp/copyright.jsp

particle. This segregation is responsible for the survival of the Pd-atop signal even for large amounts of subsequently deposited Co. The situation is schematically illustrated in the left panel of Fig. 10. A discrimination of the CO-stretching signal bound to Co-atop sites is complicated by the fact that it is near the frequency range of CO bound to Pd-bridge or particle-edge sites. An additional difficulty may be the lower dynamic dipole moment of this species, although a quantitative evaluation of this quantity is not possible. In contrast, the signal intensity from Pd-atop sites is strong and easily distinguished from other peaks in the spectra. It gives a clear example of how these sites are well preserved upon formation of bimetallic particles. The addition of only 0.1 Å Pd to 2 Å Co results in a clear absorption band from Pd-atop sites at $2105\,cm^{-1}$, which continues as more and more Pd is added. As mentioned above it is also preserved when large amounts of Co are added on top of Pd, as shown by the spectra of 3 Å Co added to 2 Å Pd particles. Since the Pd threefold site is not a clear feature at saturation coverage of CO, it cannot be used to compare the vulnerability of threefold sites to bimetallic formation. However, the coverage-dependent spectra discussed above clearly prove the expectations based on the ensemble effect to be correct.

Remarkably, the stretching frequency for CO bound to a given site is nearly independent of the bimetallic composition at low temperature (Fig. 9). However, the desorption temperature of CO is lower on the bimetallic particles than on either metal alone;[16] for example, the addition of only 0.1 Å Co to 2 Å Pd shifts the CO desorption from Pd threefold sites down from 440 to 417 K. This suggests that while the donation from the 5σ orbital of CO to the metal is changed, thus changing the binding energy, the backdonation from the metal into the $2\pi^*$ antibonding orbital of CO is almost unchanged, resulting in no change in the stretching frequency. An example of this phenomenon has been observed using ultraviolet photoemission spectroscopy (UPS), IRAS, and resonantly enhanced multiphoton ionization (REMPI) for CO interactions with Pt(111)–Ge alloy surfaces[33,34] and has been explained in terms of *d*-band filling as a result of *s*-*d* hybridization between the Pt *d*-band and Ge valence electrons. In the framework of the Blyholder model,[35] the density of states in the *d* band available for adsorption decreases upon alloy formation, and hence the charge transfer from the 5σ orbital of CO to the metal decreases, thereby decreasing the binding energy. At the same time, the relative increase in occupancy of the *d* band is negligible and has a minor effect on the reverse charge transfer from the metal *d* band to the $2\pi^*$ antibonding orbital of CO, resulting in a similar vibrational frequency on the metal or alloy.[34] Indeed, a redistribution of the density of states in the *d* band has been observed for the Co–Pd bimetallic particles with XPS.[16]

The lack of much difference in the CO stretching frequency on the bimetallic particles compared with the pure Pd or Co particles suggests that there is also little change in the CO bond strength. The implication for the Fischer–Tropsch reaction is that CO is no more easily dissociated on the Co–Pd bimetallic particles than on pure Co particles. It is believed that the surface carbide mechanism, whereby CO first dissociates and then builds CH_2 units into a chain, occurs on Co catalysts,[36] where the hydrogenation of the surface C is believed to be rate limiting. Thus, no change in CO hydrogenation rate might be expected even if there was a change in the CO bond strength on Co–Pd bimetallic particles. It is still possible that the addition of Pd facilitates the reduction of CoO,[3–5] resulting in a greater number of active sites. It is also possible that Pd enhances the rate of surface-C hydrogenation by providing more hydrogen.

IV. CONCLUSIONS

IRAS of CO was used as a surface-sensitive probe for the available binding sites of Co–Pd bimetallic particles supported on a thin alumina film. A high-coverage state attributable to an $M(CO)_n$ species is obtained on the Co particles in addition to atop sites. Bridge and threefold sites are not detected from CO stretching on the Co particles. IRAS confirms the previous conclusions[16] that sequentially deposited Co and Pd form bimetallic particles with a core-shell structure. However, it is necessary to mention that the amount of Co required to cover Pd particles is much larger than expected by simple geometric considerations due to the tendency of Pd to segregate to the surface of the bimetallic particles. Additionally, deposition of Co on top of Pd gives rise to pure Co clusters in addition to the bimetallic ones, because of the higher nucleation density of Co as compared to Pd. The IRAS measurements clearly show that atop sites are better preserved at various bimetallic compositions than higher-coordinated sites, because they are statistically less vulnerable. Finally, a combination of IRAS and TPD results shows that the stretching frequency of CO to a given site is nearly independent of the bimetallic composition while the binding energy is much more strongly altered by the environment of the adsorption site.

ACKNOWLEDGMENTS

Support for this work was provided by the Max-Planck Society and the Deutsche Forschungsgemeinschaft. A.C. thanks the Humboldt Foundation for a fellowship.

[1] D. J. Wilhelm, D. R. Simbeck, A. D. Karp, and R. L. Dickenson, Fuel Proc. Tech. **71**, 139 (2001).
[2] F. Fischer and H. Tropsch, Brennstoff-Chem. **7**, 97 (1926); H. Schulz, Appl. Catal., A **186**, 3 (1999).
[3] L. Guczi and L. Borko, Catal. Today **64**, 91 (2001).
[4] L. Guczi, L. Borko, Z. Schay, D. Bazin, and F. Mizukami, Catal. Today **65**, 51 (2001); L. Guczi, Z. Schay, G. Stefler, and F. Mizukami, J. Mol. Catal. A: Chem. **141**, 177 (1999); N. Tsubaki, S. Sun, and K. Fujimoto, J. Catal. **199**, 236 (2001).
[5] H. Idriss, C. Diagne, J. P. Hindermann, A. Kinnemann, and M. A. Barteau, in *Proceedings, 10th International Congress on Catalysis, Budapest, 1992*, edited by P. Tetenyi (Elsevier, Budapest, 1992), Vol. C, p. 2119; M. P. Kapoor, A. L. Lapidus, and A. Y. Krylova, in *Proceedings, 10th International Congress on Catalysis, Budapest, 1992*, edited by P. Tetenyi (Elsevier, Budapest, 1992), Vol. C, p. 2741; W. Juszczyk, Z. Karpinski, D. Lomot, J. Pielaszek, Z. Paal, and A. Y. Stakheev, J. Catal. **142**, 617 (1993); F. B. Noronha, M. Schmal, C. Nicot, B. Moraweck, and R. Frety, *ibid.* **168**, 42 (1997); S. Bischoff, A. Weight, K. Fujimoto, and B. Lücke, J. Mol. Catal. A: Chem. **95**, 259 (1995).
[6] M. E. Bridge and R. M. Lambert, Surf. Sci. **82**, 413 (1979); G. R. Castro and J. Küppers, *ibid.* **123**, 456 (1982).
[7] M. Gierer, H. Over, P. Rech, E. Schwarz, and K. Christmann, Surf. Sci. **380**, L201 (1997).
[8] G. W. Simmons, Y.-N. Wang, J. Marcos, and K. Klier, J. Phys. Chem. **95**,

Downloaded 28 Mar 2007 to 141.14.132.17. Redistribution subject to AIP license or copyright, see http://jcp.aip.org/jcp/copyright.jsp

4522 (1991); E. Shimada, H. Yamashita, S. Matsumoto, Y. Ikuma, and H. Ichimura, J. Mater. Sci. **34**, 4011 (1999); E. H. Voogt, A. J. M. Mens, O. L. J. Gijzeman, and J. W. Geus, Surf. Sci. **373**, 210 (1997).
[9] R. M. Jaeger, H. Kuhlenbeck, H.-J. Freund, M. Wuttig, W. Hoffmann, R. Franchy, and H. Ibach, Surf. Sci. **259**, 235 (1991).
[10] M. Frank and M. Bäumer, Phys. Chem. Chem. Phys. **2**, 3723 (2000).
[11] M. Bäumer and H.-J. Freund, Prog. Surf. Sci. **61**, 127 (1999).
[12] M. Heemeier, A. F. Carlsson, M. Naschitzki, M. Schmal, M. Bäumer, and H.-J. Freund, Angew. Chem., Int. Ed. Engl. **41**, 4073 (2002).
[13] K. H. Hansen, T. Worren, S. Stempel, E. Laegsgaard, M. Baumer, H. J. Freund, F. Besenbacher, and I. Stensgaard, Phys. Rev. Lett. **83**, 4120 (1999).
[14] T. Hill, M. Mozaffari-Afshar, J. Schmidt, T. Risse, S. Stempel, M. Heemeier, and H. J. Freund, Chem. Phys. Lett. **292**, 524 (1998).
[15] M. Bäumer, M. Frank, M. Heemeier, R. Kühnemuth, S. Stempel, and H. J. Freund, Surf. Sci. **454–456**, 957 (2000).
[16] A. F. Carlsson, M. Naschitzki, M. Bäumer, and H. J. Freund, J. Phys. Chem. B **107**, 778 (2003).
[17] T. Giessel, O. Schaff, C. J. Hirschmugl *et al.*, Surf. Sci. **406**, 90 (1998); X. Guo, J. John, and T. Yates, J. Chem. Phys. **90**, 6761 (1989).
[18] J. Lahtinen, J. Vaari, and K. Kauraala, Surf. Sci. **418**, 502 (1998); J. Lahtinen, J. Vaari, K. Kauraala, E. A. Soares, and M. A. Van Hove, *ibid.* **448**, 269 (2000).
[19] J. A. Rodriguez, Surf. Sci. Rep. **24**, 225 (1996); C. T. Campbell, Annu. Rev. Phys. Chem. **41**, 775 (1990); P. Liu and J. K. Norskov, Phys. Chem. Chem. Phys. **3**, 3814 (2001).
[20] J. Schmidt, T. Risse, H. Hamann, and H. J. Freund, J. Chem. Phys. **116**, 10861 (2002).
[21] R. M. Jaeger, J. Libuda, M. Bäumer, K. Homann, H. Kuhlenbeck, and H.-J. Freund, J. Electron Spectrosc. Relat. Phenom. **64/65**, 217 (1993).
[22] R. L. Toomes and D. A. King, Surf. Sci. **349**, 1 (1996).
[23] T. Risse, A. F. Carlsson, M. Bäumer, T. Klüner, and H.-J. Freund, Surf. Sci. (to be published).
[24] P. Hollins, Surf. Sci. Rep. **16**, 51 (1992).
[25] G. A. Beitel, A. Laskov, H. Oosterbeek, and E. W. Kuipers, J. Phys. Chem. **100**, 12 494 (1996).
[26] A. M. Bradshaw and J. Pritchard, Proc. R. Soc. London, Ser. A **316**, 169 (1970).
[27] M. J. Heal, E. C. Leisegang, and R. G. Torrington, J. Catal. **51**, 314 (1978).
[28] R. A. Gardner and R. H. Petrucci, J. Am. Chem. Soc. **82**, 5051 (1960); N. N. Kavtaradze and N. P. Sokolova, Zh. Fiz. Khim. **38**, 1004 (1964).
[29] N. Sheppard and T. T. Nguyen, in *Advances in Infrared and Raman Spectroscopy*, edited by R. J. H. Clark (Heyden, London, 1978), Vol. 5, p. 67.
[30] L. A. Hanlan, H. Huber, E. P. Kundig, B. R. McGarvey, and G. A. Ozin, J. Am. Chem. Soc. **97**, 7054 (1975).
[31] K. Wolter, O. Seiferth, H. Kuhlenbeck, M. Bäumer, and H.-J. Freund, Surf. Sci. **399**, 190 (1998).
[32] M. Krawczyk, L. Zommer, B. Lesiak, and A. Jablonski, Surf. Interface Anal. **25**, 356 (1997).
[33] K. Fukutani, T. T. Magkoev, Y. Murata, M. Matsumoto, T. Kawauchi, T. Magome, Y. Tezuka, and S. Shin, J. Electron Spectrosc. Relat. Phenom. **88**, 597 (1998); K. Fukutani, Y. Murata, J. Brillo, H. Kuhlenbeck, H. J. Freund, and M. Taguchi, Surf. Sci. **464**, 48 (2000).
[34] T. T. Magkoev and Y. Murata, Tech. Phys. **47**, 752 (2002).
[35] G. Blyholder, J. Phys. Chem. **68**, 2772 (1964).
[36] B. H. Davis, Fuel Proc. Tech. **71**, 157 (2001).

Downloaded 28 Mar 2007 to 141.14.132.17. Redistribution subject to AIP license or copyright, see http://jcp.aip.org/jcp/copyright.jsp